


# Mitochondrial uncoupling attenuates sarcopenic obesity by enhancing skeletal muscle mitophagy and quality control

Wagner S. Dantas<sup>1</sup>, Elizabeth R.M. Zunica<sup>1</sup>, Elizabeth C. Heintz<sup>1</sup>, Bolormaa Vandanmagsar<sup>1</sup>, Z. Elizabeth Floyd<sup>2</sup>, Yongmei Yu<sup>2</sup>, Hisashi Fujioka<sup>3,4</sup>, Charles L. Hoppel<sup>1,4,5</sup>, Kathryn P. Belmont<sup>1</sup>, Christopher L. Axelrod<sup>1\*</sup> & John P. Kirwan<sup>1\*</sup> 

<sup>1</sup>Integrated Physiology and Molecular Medicine Laboratory, Pennington Biomedical Research Center, Baton Rouge, LA, USA; <sup>2</sup>Ubiquitin Biology Laboratory, Pennington Biomedical Research Center, Baton Rouge, LA, USA; <sup>3</sup>Cryo-Electron Microscopy Core, Case Western Reserve University, Cleveland, OH, USA; <sup>4</sup>Center for Mitochondrial Diseases, Case Western Reserve University of School of Medicine, Cleveland, OH, USA; <sup>5</sup>Department of Pharmacology, Case Western Reserve University, Cleveland, OH, USA

## Abstract

**Background** Sarcopenic obesity is a highly prevalent disease with poor survival and ineffective medical interventions. Mitochondrial dysfunction is purported to be central in the pathogenesis of sarcopenic obesity by impairing both organelle biogenesis and quality control. We have previously identified that a mitochondrial-targeted furazano [3,4-b]pyrazine named BAM15 is orally available and selectively lowers respiratory coupling efficiency and protects against diet-induced obesity in mice. Here, we tested the hypothesis that mitochondrial uncoupling simultaneously attenuates loss of muscle function and weight gain in a mouse model of sarcopenic obesity.

**Methods** Eighty-week-old male C57BL/6J mice with obesity were randomized to 10 weeks of high fat diet (CTRL) or BAM15 (BAM15; 0.1% w/w in high fat diet) treatment. Body weight and food intake were measured weekly. Body composition, muscle function, energy expenditure, locomotor activity, and glucose tolerance were determined after treatment. Skeletal muscle was harvested and evaluated for histology, gene expression, protein signalling, and mitochondrial structure and function.

**Results** BAM15 decreased body weight ( $54.0 \pm 2.0$  vs.  $42.3 \pm 1.3$  g,  $P < 0.001$ ) which was attributable to increased energy expenditure ( $10.1 \pm 0.1$  vs.  $11.3 \pm 0.4$  kcal/day,  $P < 0.001$ ). BAM15 increased muscle mass ( $52.7 \pm 0.4$  vs.  $59.4 \pm 1.0\%$ ,  $P < 0.001$ ), strength ( $91.1 \pm 1.3$  vs.  $124.9 \pm 1.2$  g,  $P < 0.0001$ ), and locomotor activity ( $347.0 \pm 14.4$  vs.  $432.7 \pm 32.0$  m,  $P < 0.001$ ). Improvements in physical function were mediated in part by reductions in skeletal muscle inflammation (interleukin 6 and gp130, both  $P < 0.05$ ), enhanced mitochondrial function, and improved endoplasmic reticulum homeostasis. Specifically, BAM15 activated mitochondrial quality control (PINK1-ubiquitin binding and LC3II,  $P < 0.01$ ), increased mitochondrial activity (citrate synthase and complex II activity, all  $P < 0.05$ ), restricted endoplasmic reticulum (ER) misfolding (decreased oligomer A11 insoluble/soluble ratio,  $P < 0.0001$ ) while limiting ER stress (decreased PERK signalling,  $P < 0.0001$ ), apoptotic signalling (decreased cytochrome C release and Caspase-3/9 activation, all  $P < 0.001$ ), and muscle protein degradation (decreased 14-kDa actin fragment insoluble/soluble ratio,  $P < 0.001$ ).

**Conclusions** Mitochondrial uncoupling by agents such as BAM15 may mitigate age-related decline in muscle mass and function by molecular and cellular bioenergetic adaptations that confer protection against sarcopenic obesity.

**Keywords** Sarcopenia; Obesity; Ageing; Bioenergetics; Mitochondrial uncoupling; BAM15

Received: 7 December 2021; Revised: 28 January 2022; Accepted: 21 February 2022

\*Correspondence to: John P. Kirwan and Christopher L. Axelrod, Integrated Physiology and Molecular Medicine Laboratory, Pennington Biomedical Research Center, 6400 Perkins Road, Baton Rouge, LA 70808, USA. Email: john.kirwan@pbrc.edu; christopher.axelrod@pbrc.edu  
Wagner S. Dantas and Elizabeth R. M. Zunica contributed equally to this work.

## Introduction

Adults over the age of 65 constitute the largest and most rapidly expanding demographic globally.<sup>1</sup> Age-related loss of skeletal muscle mass and function, known as sarcopenia, is a significant contributor to physical immobility, frailty, malnutrition, and reduced quality of life.<sup>2</sup> Sarcopenia is a strong predictor of hospitalization, institutionalization, and mortality in older adults.<sup>3</sup> Obesity is observed in ~35% of adults over 65 and exacerbates sarcopenia by accelerating fat accumulation and lowering physical activity.<sup>4</sup> Adults with sarcopenic obesity are at high risk for long-term disability, worsened quality of life, and death, representing a serious public health concern.<sup>4</sup> As such, interventions that prevent, delay, or reverse the causes and consequences of sarcopenic obesity may reduce morbidity and enhance lifespan in older adults. Mitochondria are the primary site of energy production, a process maintained by the coupling of electron transfer and proton pumping to gradient-driven synthesis of ATP, and thus highly influence muscle function. Ageing is associated with several mitochondrial derangements including reduction of volume, enzymatic activity, respiratory function, membrane dynamics, and quality control.<sup>5,6</sup> Obesity exacerbates age-related mitochondrial stress by increasing substrate flow, oxidative stress, inflammation, and endoplasmic reticulum (ER) stress, exacerbating the decline in structure and function as well as protein degradation.<sup>7</sup> Interestingly, pharmacologic and genetic lowering of mitochondrial coupling efficiency confers lifespan extension in rodents<sup>8</sup> and insects.<sup>9</sup> However, the effects of mitochondrial uncoupling in the context of sarcopenic obesity remain entirely unknown. We have previously reported a mitochondrial protonophore named BAM15 ((2-fluorophenyl){6-[(2-fluorophenyl)amino](1,2,5-oxadiazolo[3,4-e]pyrazin-5-yl)}amine) that prevents diet-induced obesity and preserves lean mass to a greater extent than dietary restriction in young mice.<sup>10</sup> Here, we identified that sustained mitochondrial uncoupling concomitantly prevented age-related deterioration of muscle function. We observed that BAM15-mediated mitochondrial uncoupling restored mitochondrial quality control and performance, thereby enhancing mitochondria-ER crosstalk and lowering systemic and muscular inflammation. Taken together, our findings indicate that limiting coupling efficiency may provide therapeutic value in the treatment of sarcopenic obesity.

## Methods

### *Animal care*

Male C57BL/6J mice ( $n = 12$ ) were purchased from Jackson Laboratory, multihoused, and kept on a standard chow diet (Purina 5015). At 72 weeks of age, mice were single housed at 27–28°C with a relative humidity of  $50 \pm 10\%$  on a 12 h

of light:dark cycle with ad libitum access to food and water. Animals were fed a high fat diet (HFD; 60% fat, 20% protein, and 20% carbohydrate, HFD Research Diets) during treatment. All procedures involving animals were approved by the Institutional Animal Care and Use Committee.

### *Experimental design*

At 80 weeks of age, animals were randomized by body weight to 10 weeks of HFD (CTRL,  $n = 6$ ) or HFD + BAM15 (BAM15; 0.1% w/w BAM15,  $n = 6$ ). One animal died during treatment and was excluded from analysis. The dosing strategy and delivery for BAM15 was adapted from previous work in wildtype C57BL/6J mice.<sup>10,11</sup> Body temperature, body weight, and food intake were measured daily. At study end, mice were euthanized using isoflurane followed by rapid cervical dislocation.

### *Body temperature*

Body temperature was recorded via infrared thermometry during weighing (Fluke 572-2 Infrared Thermometer; Fluke, Everett, WA, USA) as described previously.<sup>10</sup>

### *Body composition*

Body composition was assessed 10 weeks after treatment via nuclear magnetic resonance using an LF110 BCA Analyser (Bruker Corporation, Billerica, MA, USA) as described previously.<sup>10</sup>

### *Metabolic chamber study*

Whole-body energy expenditure, oxygen consumption, carbon dioxide production, body weight, food intake, and physical activity were monitored over a 7-day period in a metabolic chamber (Sable Systems) after treatment as described previously.<sup>10</sup>

### *Intraperitoneal glucose tolerance test*

Glycaemic control was assessed by intraperitoneal injection (2 g/kg body weight) and subsequent measures of glucose as described previously.<sup>10</sup> Whole blood was additionally collected for assessment of fasting insulin (Mercodia) and C-peptide (Crystal Chem) by ELISA according to the manufacturer's instruction.

### Grip strength

Peak muscular force was determined using a commercially available Grip Strength Meter (Bioseb). Briefly, mice were held by the base of the tail and allowed to grasp the wire grid with all limbs. After the animal grasped the grid, the experimenter pulled backwards until grip was lost. Grip strength was quantified as the average of three trials with 1–2 min rest between trials, repeated on four different days.

### Biochemical measurements

Blood samples were obtained by cardiac puncture in animals under terminal anaesthesia into a capillary tube coated with K3-EDTA. Plasma was isolated by centrifugation at 2000g for 20 min at 4°C and stored at –80°C until assay. Tumour necrosis factor alpha (TNF- $\alpha$ ), interleukin 6 (IL-6), IL-1 $\beta$ , interferon gamma, and interleukin 10 concentrations were determined by bead-based multiplex assay (Bio-Plex Pro™, Biorad) according to manufacturer's instructions.

### RNA extraction and quantitative real-time PCR

Gastrocnemius muscle was homogenized in TRIzol™, and total RNA was isolated according to the manufacturer's instructions. Quantitative real-time qPCR and quantification was performed as described previously.<sup>10</sup> Expression was normalized to beta-actin ( $\beta$ -actin). Primer sequences are provided in Supporting Information, Table S1.

### Mitochondrial isolation

Mitochondrial isolation was performed as described previously.<sup>12</sup> Briefly, gastrocnemius muscle (~50 mg) was minced and homogenized in a Wheaton Glass tube with 2 mL of cold isolation buffer with phosphatase and protease inhibitors. After centrifugation at 600g for 10 min, supernatant containing the mitochondria pellet was washed at 7000g for 10 min. Mitochondria and cytosol were stored in –80°C for subsequent analysis.

### Immunoblotting

Gastrocnemius and soleus proteins were solubilized and detected by immunoblotting as described previously.<sup>13</sup> Expression was normalized relative to total protein and/or endogenous controls (VDAC) as noted in the figure legends. Phosphorylated proteins were normalized relative to both total protein and loading controls. Antibodies are displayed in Table S1.

### Immunoprecipitation assay

Mitochondrial pellets were lysed (20 mM of Tris pH 7.4, 137 mM of NaCl, 1% of NP-40, 1 mM of PMSF, 20% of glycerol, 10 mM of sodium fluoride, 1 mM of sodium orthovanadate, 2  $\mu$ g/mL of leupeptin and aprotinin) in the presence of protease and phosphatase inhibitors (Sigma) and centrifuged at 12 000g for 15 min at 4°C. Mitochondrial lysates were incubated with a polyclonal PINK1 antibody followed by incubation with protein A/G agarose beads (Santa Cruz Biotechnology) overnight at 4°C. Proteins were separated by SDS-PAGE, transferred, and incubated overnight with ubiquitin (P37) antibody followed by HRP-tagged secondary antibody.

### Actin cleavage and insoluble protein aggregates isolation

Caspase-3-generated 14-kDa actin fragments and insoluble protein aggregates were determined in soleus muscle. Tissue (~15 mg) was homogenized on ice-cold buffer (10% of glycerol, 10 mM of Tris pH 7.4, 1% of Triton-X 100, 150 mM of NaCl with protease inhibitors) and centrifuged at 15 000g for 20 min at 4°C. The supernatant was transferred to a chilled tube, and the pellet (insoluble fraction) was washed twice with 500  $\mu$ L of PBS with protease inhibitors and lysed with detergent buffer (10 mM of Tris pH 7.4, 1% of Triton-X 100, 150 mM of NaCl, 10% of glycerol, 4% of SDS and protease inhibitors). Samples were sonicated for 20 s, chilled on ice for 30 min, and centrifuged for 30 s at 6000g. Final supernatant and pellet fractions were mixed with Laemli two times sample loading buffer, denatured at 100°C for 20 min, and run on 10% (Oligomer A11) and 15% (14-kDa actin fragment) SDS-PAGE gels.<sup>13</sup> Anti  $\beta$ -actin produced in rabbit using C-terminal actin fragment (C11 peptide attached to multiple antigen peptide backbone) was used to recognize the 14-kDa fragment.

### Myofibre cross-sectional area

Gastrocnemius tissue was embedded in optimal cutting temperature compound, frozen, and stored at –80°C until analysis as previously described.<sup>13</sup> Transverse serial cross-sections (10  $\mu$ m) were obtained using a cryostat maintained at –25°C, mounted onto glass microscope slides, and stained with haematoxylin–eosin. Images were captured at  $\times$ 20 magnification and quantified using ImageJ.

### Transmission Electron microscopy

Red gastrocnemius muscle was collected at the time of necropsy and assessed for mitochondrial ultrastructure and

content as described previously.<sup>10</sup> Briefly, small pieces of tissue were fixed by immersion in Karnovsky's solution, rinsed in 0.1 M of phosphate buffer pH 7.4, and then postfixed in a mixture of 2% osmium tetroxide and 3% potassium ferricyanide. Thin sections were stained with acidified uranyl acetate followed by a modification of Sato's triple lead stain. Mitochondrial content was determined by manual tracing of clearly discernible outlines of mitochondria and quantified using threshold analysis using ImageJ.

### Mitochondrial DNA

Soleus muscle was lysed (10 mM of Tris pH 7.4, 100 mM of NaCl, 10 mM of EDTA, 10% of SDS) in the presence of proteinase K (ThermoScientific) overnight at 55°C. DNA was extracted by phenol-chloroform and centrifuged at 14 000 rpm 10 min at 4°C. Supernatant was collected and centrifuged at 14 000 rpm for 10 min. The pellet was cleaned in ice-cold 100% ethanol and suspended in 100 µL of TE buffer (10 mM of Tris pH 7.4, 1 mM of EDTA). RT-qPCR was performed as previously described<sup>10</sup> using mitochondrial encoded cytochrome C oxidase subunit II (*mtCox2*) and nuclear-encoded 18S ribosomal (*18S*) genes.

### Mitochondrial enzyme activity

Mitochondrial enzyme activity was determined as described previously.<sup>14</sup> Briefly, muscle tissue (~50 mg) was powdered and lysed in 5% cholate. Complex II activity was measured as the thenoyltrifluoroacetone (TTFA)-sensitive succinate-2,6 dichlorophenol-indophenol (DCPIP) reductase and total complex II determined with coenzyme Q1 added. Antimycin A-sensitive decylubiquinol cytochrome C reductase (complex III) was utilized to determine the activity of complex III. Cytochrome C oxidase (complex IV) activity was measured as the cyanide-sensitive rate of reduced cytochrome C oxidation. Citrate synthase activity was determined by the formation of citrate in the presence of acetyl-CoA before and after addition of oxaloacetate.

### Statistical analysis

All data are expressed as means ± standard error of the mean (SEM) unless otherwise stated. Prism 9 software was used for testing statistical significance. Normality of the data was assessed by Kolmogorov–Smirnov. Two-way ANOVA followed by post hoc tests and unpaired Student's *t*-tests were used to compare quantitative variables where appropriate. Between-group differences in energy expenditure were determined using a generalized linear model with total body mass as a covariate using CalR as described previously.<sup>15</sup> Significance was set a priori at  $P \leq 0.05$ .

## Results

### *Mitochondrial uncoupling prevents diet-induced obesity and improves glucose tolerance in aged mice*

To investigate the role of bioenergetic efficiency in the regulation of sarcopenic obesity, 80-week-old male C57BL/6J mice with obesity were randomized to 10 weeks of either CTRL or BAM15. We observed that BAM15 conferred sustained protection against diet-induced weight gain compared to CTRL, consistent with previous observations in young mice<sup>10,11</sup> (Figure 1A). Food intake was comparable between BAM15 and CTRL animals despite the reduction in body weight (Figure 1B). Differences in total body weight were attributable to a reduction in fat mass, with decreased inguinal and gonadal white adipose tissue (iWAT and gWAT, respectively) mass with BAM15 compared with CTRL (Figure 1C). Next, we sought to determine whether prevention of diet-induced obesity was associated with improved glucose clearance. BAM15 reduced fasting and 120-min plasma glucose following intraperitoneal glucose injection but did not alter total area under the curve for glucose compared with CTRL (Figure 1D). BAM15-treated animals displayed favourable improvements in fasting plasma insulin, C-peptide, hepatic extraction, and HOMA-IR (Figure 1E–F). Overall, these data suggest that BAM15-induced mitochondrial uncoupling prevents diet-induced obesity, improves glucose homeostasis, and restores insulin sensitivity in aged mice.

### *Mitochondrial uncoupling preserves muscle mass and function in aged mice*

Given that body weight is intimately coupled to physical performance in the context of ageing,<sup>16</sup> we sought to determine the role of BAM15-mediated mitochondrial uncoupling in the regulation of muscle mass and function. We observed that lean mass and weight of the gastrocnemius muscle normalized to tibia length were increased with BAM15 compared with CTRL (Figure 2A). Myofibre cross-sectional area (fCSA) was increased with BAM15 compared with CTRL (Figure 2B). Functionally, BAM15-treated animals displayed improved muscular strength over the course of repeated measurements (Figure 2C), which was also associated with increased locomotion compared with CTRL (Figure 2D). To determine whether the maintenance of muscle mass and reductions in body weight following BAM15 treatment was associated with alterations in energy expenditure, animals were placed in a metabolic chamber and evaluated over 7 days. Energy expenditure was increased with BAM15, driven by increased oxygen consumption during the active dark phase with no difference during the resting light phase (Figure 2E). Given the

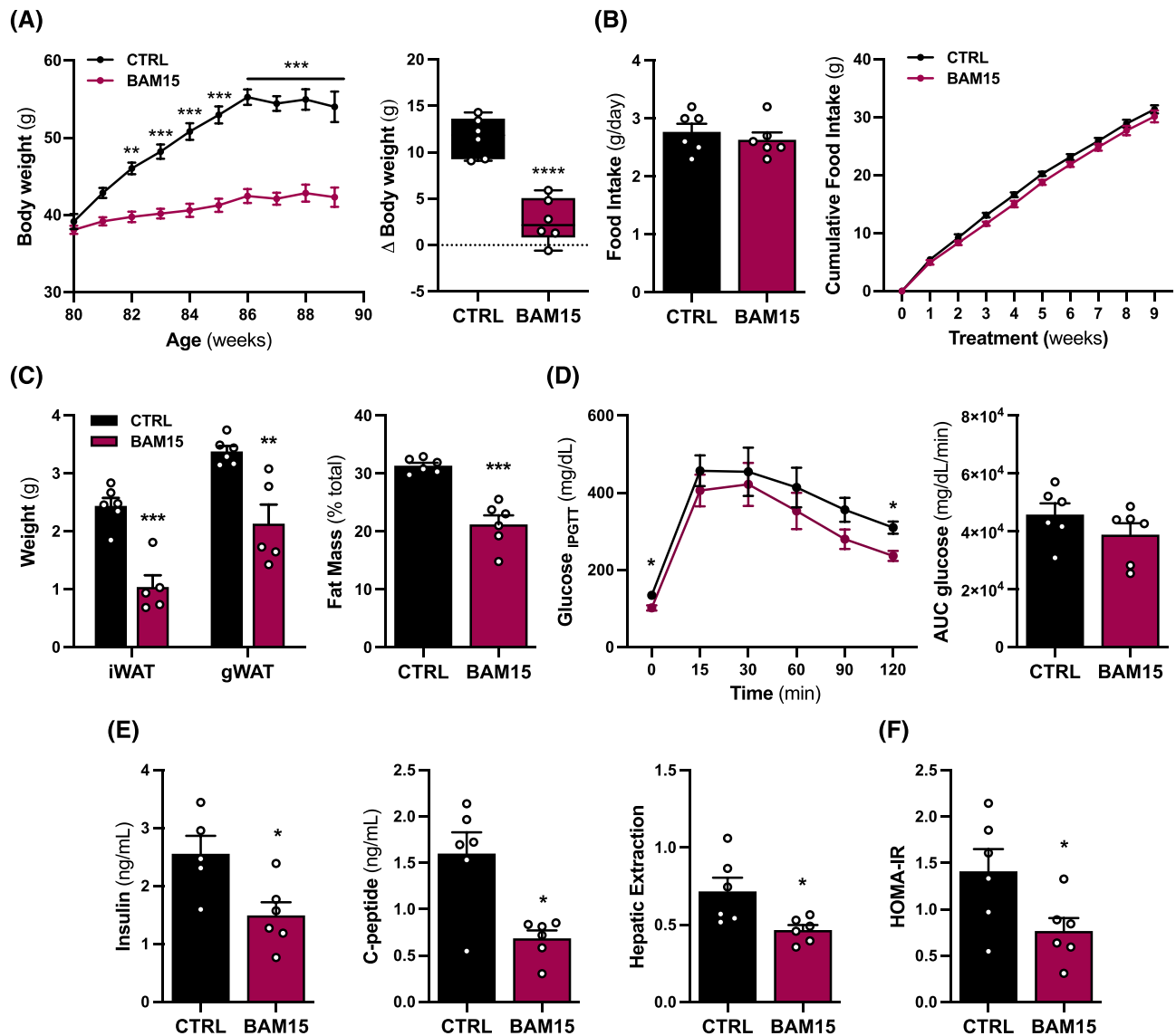


**Figure 1** Mitochondrial uncoupling prevents diet-induced obesity and improves glucose tolerance in aged mice. (A) Cumulative body weight and delta (post-pre) body weight changes; (B) average and cumulative food intake; (C) inguinal and gonadal white adipose tissue (iWAT and gWAT, respectively) weight and total fat mass; (D) plasma glucose concentrations at 0, 15, 30, 60, 90, and 120 min following intraperitoneal injection of glucose and total area under the curve (AUC) of glucose; (E) fasting plasma insulin and plasma C-peptide and hepatic extraction; and (F) whole-body homeostatic model of insulin resistance (HOMA-IR). Data are expressed as mean  $\pm$  SEM with exception to panel A (right) which is displayed as a box (mean  $\pm$  95% CI) and whiskers (minimum to maximum values) plot. Repeated measures in panels (A), (B), and (D) were assessed by two-way repeated measures ANOVA with Tukey's multiple comparisons. Two-group comparisons in panels (A), (B), (C), (D), (E), and (F) were assessed by unpaired Student's *t*-test. \**P* < 0.05, \*\**P* < 0.01, \*\*\**P* < 0.001, and \*\*\*\**P* < 0.0001 indicate statistical significance for between-group comparisons, respectively.

muscular improvements, we then sought to investigate mechanisms whereby BAM15 maintains muscle mass and function. We observed a significant increase in the fast-twitch muscle myosin heavy chain type 2 (MyHCII) but not the slow-twitch type I (MyHCI) protein expression with BAM15 compared with CTRL (Figure 2F). Taken together, these data suggest that BAM15-mediated mitochondrial uncoupling preserves skeletal muscle mass and function in aged mice, and these adaptations are linked to increased fast-twitch fibre expression and energy expenditure.

### *Mitochondrial uncoupling attenuates IL-6/STAT3-induced systemic and skeletal muscle inflammation in aged mice*

Based on the observations that BAM15 preserves muscle mass and function, we sought to investigate the effect of BAM15 on systemic inflammation and muscle-specific cytokine expression in aged mice. BAM15 treatment decreased circulating TNF- $\alpha$ , interferon gamma, interleukin 6 (IL-6), and interleukin 10, whereas IL-1 $\beta$  remained unchanged com-

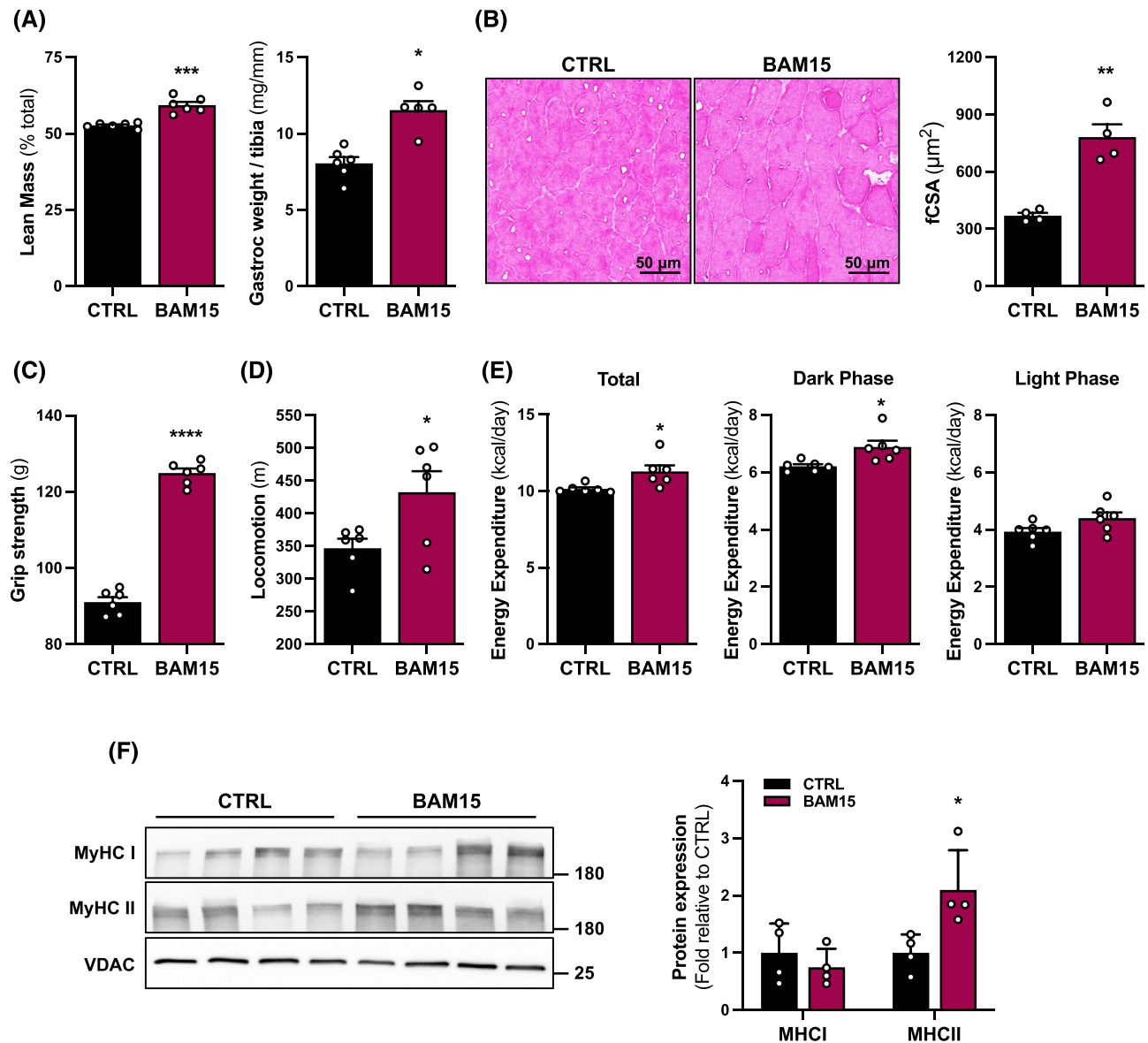


**Figure 2** Mitochondrial uncoupling preserves skeletal muscle mass and function in aged mice. (A) Lean mass and gastrocnemius (gastroc) weight normalized to tibia length. (B) Representative haematoxylin–eosin (H&E) staining of gastrocnemius muscle (scale = 50  $\mu$ m) and quantification of fibre cross-sectional area (fCSA). (C) Grip strength averaged over four repeated trials and (D) spontaneous physical movement over a 7-day period. (E) Total, dark, and light phase energy expenditure averaged over a 5-day period. (F) Representative bands of MyHC I, MyHC II, and VDAC from gastroc tissue extracts and quantification of protein expression. All comparisons were assessed by unpaired Student's *t*-test. \**P* < 0.05, \*\**P* < 0.01, \*\*\**P* < 0.001, and \*\*\*\**P* < 0.0001 indicate statistical significance for between-group comparisons, respectively.

pared with CTRL (Figure 3A). In addition, we evaluated two major markers of immune cell infiltration and macrophage activation in skeletal muscle. BAM15 downregulated *F4/80* and *Cd45*, whereas *Cd64* and *Cd68* expression remained unaltered (Figure 3B). We also assessed the expression of cytokine-related signal transduction proteins in skeletal muscle. Consistent with what we observed in the circulation, BAM15 decreased muscle cytokine protein expression of IL-6 along with one of its transmembrane receptors, glycoprotein 130 (gp130) with BAM15, with no change in IL-1 $\beta$  com-

pared with CTRL (Figure 3C). We evaluated two major mitogen-activated protein kinase (MAPK) cascades that transduce extracellular signals related to inflammation into skeletal muscle. There was no difference in c-Jun N-terminal kinase phosphorylation, whereas extracellular signal-regulated kinase 1/2 (ERK 1/2) phosphorylation was diminished with BAM15 (Figure 3C). Furthermore, the difference found in fast-twitch muscle fibres was not associated with activation of the mechanistic target of rapamycin (mTOR) pathway, a master regulator of anabolic signalling (Figure 3D). However,

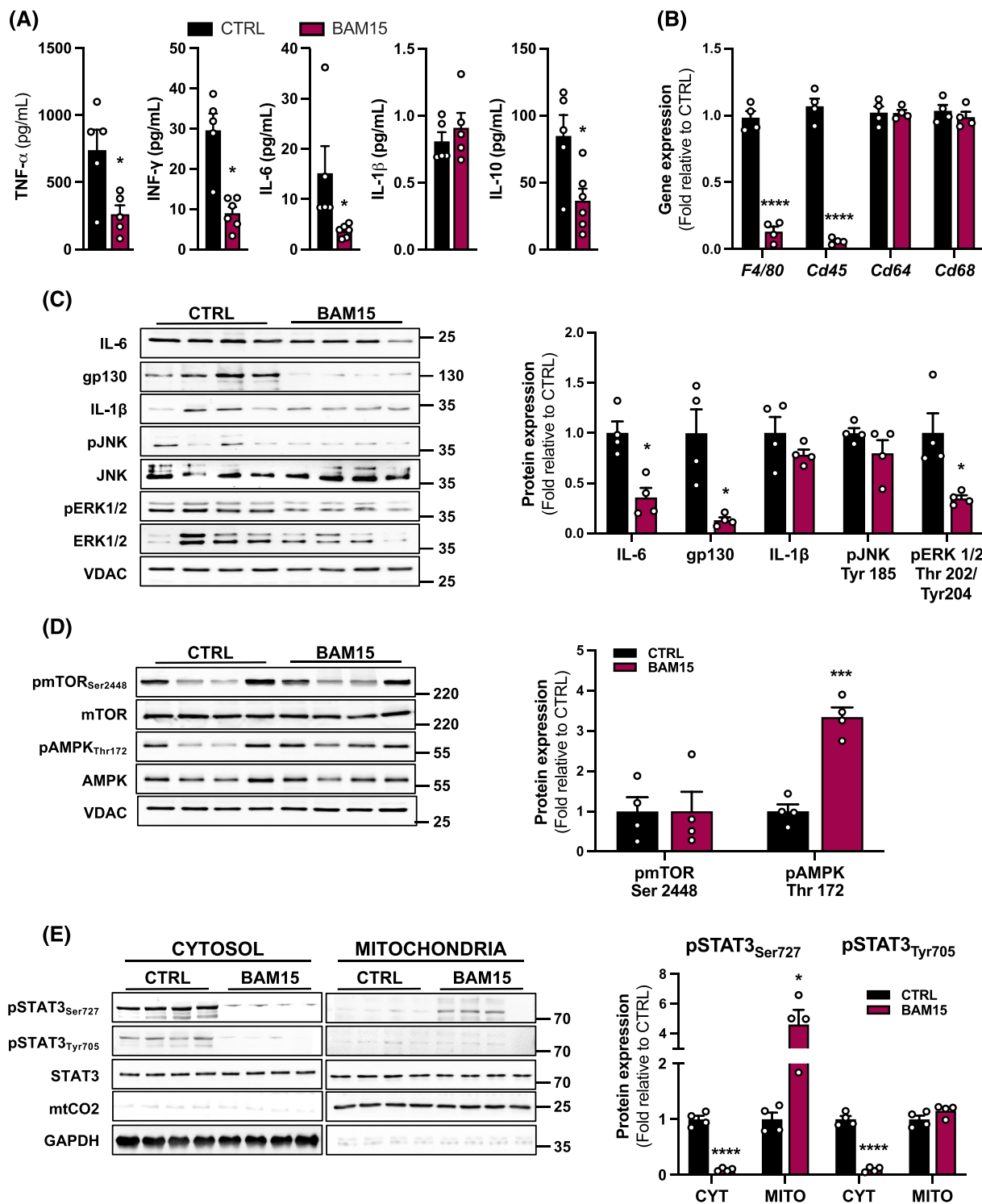


**Figure 3** Mitochondrial uncoupling attenuates age-related IL-6/STAT3-induced systemic and skeletal muscle inflammation in aged mice. (A) Plasma concentrations of TNF- $\alpha$ , INF- $\gamma$ , IL-6, IL-1 $\beta$ , and IL-10. (B) Gene expression of *F4/80*, *Cd45*, *Cd64*, and *Cd68* normalized to  $\beta$ -actin. (C) Representative bands of IL-6, gp130, IL-1 $\beta$ , JNK<sub>Thr183/Tyr185</sub>, ERK1/2<sub>Thr202/Tyr204</sub>, and VDAC from tissue extracts and quantification of protein expression. (D) Representative bands of pmTOR<sub>Ser2448</sub>, total mTOR, pAMPK<sub>Thr172</sub>, total AMPK, and VDAC from gastroc tissue extracts and quantification of protein expression. (E) Representative bands of pSTAT3<sub>Ser727</sub>, pSTAT3<sub>Tyr705</sub>, total STAT3, mtCO2, and GAPDH from the cytosolic and mitochondrial compartments of tissue extracts and quantification of protein expression. Data are expressed as mean  $\pm$  SEM. All comparisons were assessed by unpaired Student's *t*-test. \* $P < 0.05$  and \*\*\*\* $P < 0.0001$  indicate statistical significance for between-group comparisons, respectively.

consistent with our previous findings that BAM15 protected against diet-induced obesity in an AMP-activated protein kinase (AMPK) -dependent manner,<sup>10</sup> we observed an increase in AMPK phosphorylation with BAM15 compared with CTRL (Figure 3D). During inflammation, pro-inflammatory factors, such as IL-1 $\beta$  and IL-6, can activate cell surface receptors that stimulate ERK 1/2 phosphorylation.<sup>17,18</sup> We observed that ERK 1/2 activation and IL-6 expression were decreased after BAM15 treatment with no change in IL-1 $\beta$  expression, suggesting that ERK 1/2 activation in muscle inflammation was mediated through IL-6, in our model. To clarify mechanisms whereby mitochondrial uncoupling lowers muscle inflammation, we measured signal transducer and activator of transcription 3 (STAT3) phosphorylation and intracellular mitochondrial localization, the downstream target of IL-6. Cytosolic STAT3 phosphorylation at Ser727 and Tyr705 was decreased with BAM15 compared with CTRL (Figure 3E). Conversely, mitochondrial STAT3 phosphorylation at Ser727 was increased with BAM15 compared with CTRL (Figure 3E). Overall, these data suggest that BAM15-mediated mitochondrial uncoupling reduces systemic and skeletal muscle tissue inflammation in part by regulating IL-6/IL6R/gp130-signalling, consequently decreasing ERK-pathway and activating mitochondrial STAT3-pathway in skeletal muscle.

### *Mitochondrial uncoupling enhances mitochondrial quality control and respiratory activity in aged mice*

STAT3 is constitutively present in the mitochondrial matrix and regulates the rate of electron transfer.<sup>19</sup> To better understand if mitochondrial STAT3 activation corresponds to changes in mitochondrial dynamics and function in aged mice, we first assessed protein expression of several markers related to mitochondrial proteostasis in isolated mitochondria. We observed that BAM15 increased the expression of ATP synthase but no other mitochondrial complexes, compared with CTRL (Figure 4A). Additionally, BAM15 increased protein expression of the transcriptional coactivator peroxisome proliferator-activated receptor- $\gamma$  coactivator-1 $\alpha$  (PGC-1 $\alpha$ ) (Figure 4A–B), a master regulator of mitochondrial biogenesis and mitochondrial DNA content (Figure 4C). We subsequently conducted electron microscopy analysis of muscle mitochondria and observed that BAM15 increased mitochondrial content, favouring larger, more densely packed tubular shaped networks (Figure 4D–E). To confirm whether mitochondrial biogenesis contributes to increased function, we analysed enzymatic activity of citrate synthase and mitochondrial complexes II, III, and IV. BAM15 treatment increased citrate synthase and mitochondrial complex II activity, without significant differences for mitochondrial complexes III and IV activity (Figure 4F). Taken together, BAM15 increases

mitochondrial ATP synthase expression, mitochondrial biogenesis, and activity in skeletal muscle of aged mice.

Given that loss of proteostasis and mitochondrial dysfunction are hallmarks of ageing,<sup>20</sup> we isolated mitochondria and assessed protein expression of components of mitochondrial dynamics. Although, dynamin-1-like protein (DRP1) was not changed, we observed changes in other fission mediators with a decrease in mitochondrial outer membrane protein 2 (Mid49), mitochondrial outer membrane protein 1 (Mid51), and mitochondrial fission 1 (FIS1) (Figure 5A–B). With respect to mediators of mitochondrial fusion, BAM15 treatment increased the expression of the outer mitochondrial membrane protein, mitofusin 2 (MFN2), but decreased the expression of the inner mitochondrial membrane protein, dynamin like GTPase (OPA1) (Figure 5A and C). Interestingly, expression of the mitochondrial quality control proteins PTEN-induced kinase 1 (PINK1) was increased with BAM15 compared with CTRL, whereas Parkin was unaltered (Figure 5A and C). Mitophagy marker expression was also increased in response to BAM15 with an increase in the microtubule-associated protein 1 light chain 3 (LC3) ratio of LC3II to LC3I isoforms (Figure 5A–C). From these data, we concluded that BAM15 decreased mitochondrial fission and increased mitochondria quality control signalling in aged skeletal muscle. Mitochondrial quality control proteins, such as PINK1, are usually ubiquitin dependent. Because we observed a significant increase in PINK1 protein expression in isolated mitochondria from skeletal muscle, we sought to confirm that ubiquitination is a primary mechanism whereby BAM15 triggers mitochondrial quality control and mitophagy in muscle. These observations were supported by a BAM15-mediated increase in ubiquitination in total lysates and isolated mitochondria (Figure 5D–E). This was further corroborated by increased ubiquitin-PINK1 protein–protein interaction (Figure 5F). These data suggest that BAM15 drives PINK1 ubiquitination to facilitate mitochondrial quality control in aged muscle. In summary, the data support the view that BAM15-related improvements in muscle function may contribute to increases in mitochondrial content and improvements in quality control and function.

### *Mitochondrial uncoupling reduces skeletal muscle ER stress, apoptotic signalling, and muscle protein degradation in aged mice*

Mitochondrial functions are intricately regulated by the ER.<sup>21</sup> Certain conditions, such as obesity and ageing, disrupt ER homeostasis and lead to the accumulation of unfolded or misfolded proteins within the ER lumen.<sup>22</sup> To determine if ER stress response is attenuated by BAM15, we first analysed the protein expression of an ER transmembrane stress sensor and downstream signalling proteins. BAM15 decreased protein kinase R (PKR)-like endoplasmic reticulum kinase (PERK)



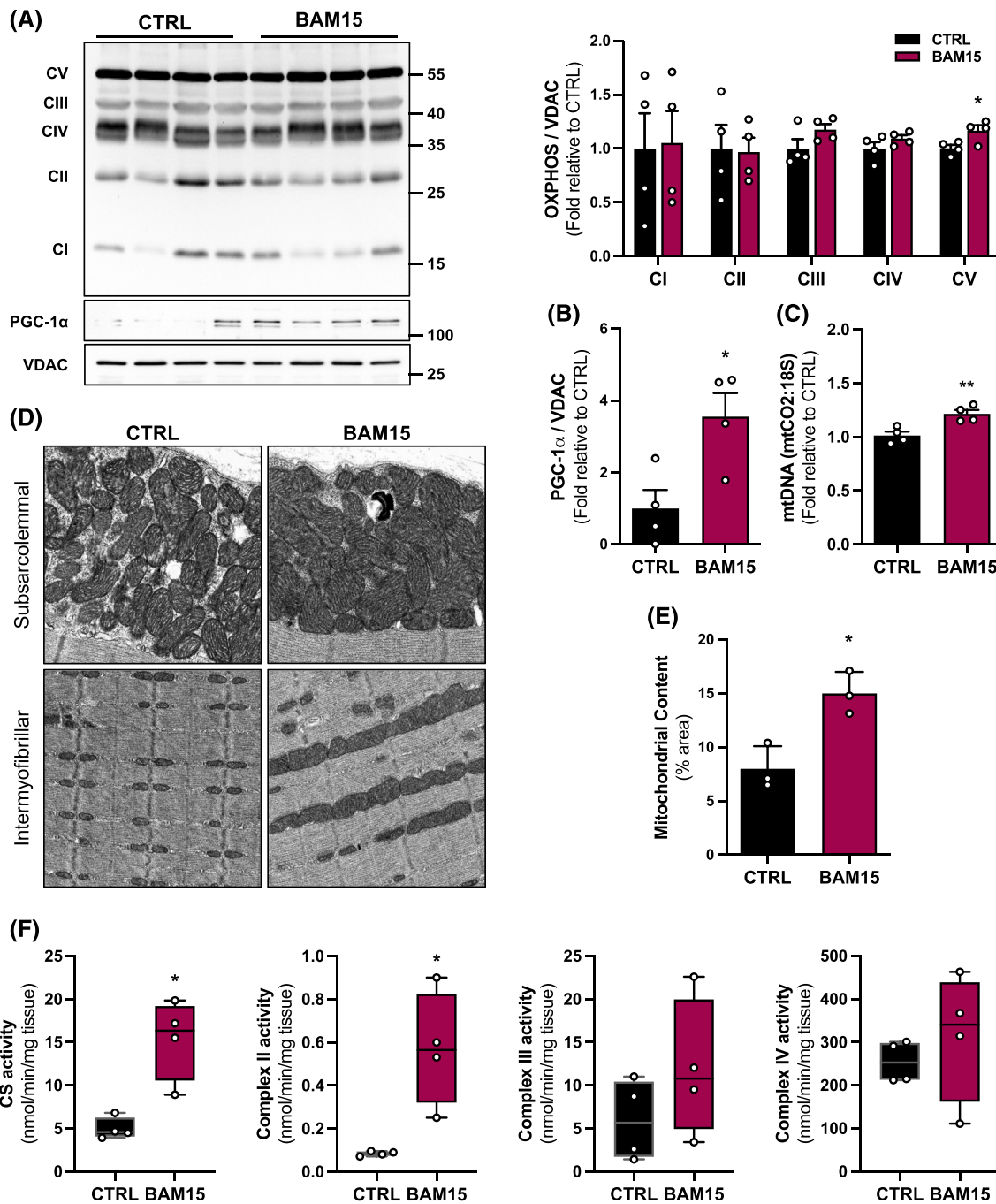


**Figure 4** Mitochondrial uncoupling enhances skeletal muscle mitochondrial biogenesis and respiratory activity in aged mice. (A) Representative bands of respiratory complex V (CV), III (CIII), IV (CIV), II (CII), and I (CI), PGC-1 $\alpha$ , and VDAC and (A–B) quantification of protein expression. (C) Mitochondrial DNA (mtDNA) content quantified as the expression of mitochondrial cytochrome C oxidase subunit 2 (*mtCO2*) normalized to 18S (*18S*). (D) Representative transmission electron micrographs of subsarcolemmal and intermyofibrillar mitochondria and (E) quantification of mitochondria content from electron micrographs. (F) Enzymatic activity of citrate synthase, complex II, complex III, and complex IV normalized to tissue wet weight. All comparisons were assessed by unpaired Student's *t*-test. \**P* < 0.05 and \*\**P* < 0.01 indicate statistical significance for between-group comparisons, respectively.

protein expression (Figure 6A–B). This corresponded to a decrease in the signalling cascade including reduced eukaryotic translation initiation factor 2A (eIF2) activation by BAM15 compared with CTRL (Figure 6A–B). Furthermore, protein ex-

pression of activating transcription factor 4 (ATF4), a potent transcription factor, was decreased by BAM15 compared with CTRL without changes in activating transcription factor 3 (ATF3) (Figure 6A–B). Additionally, we found that BAM15

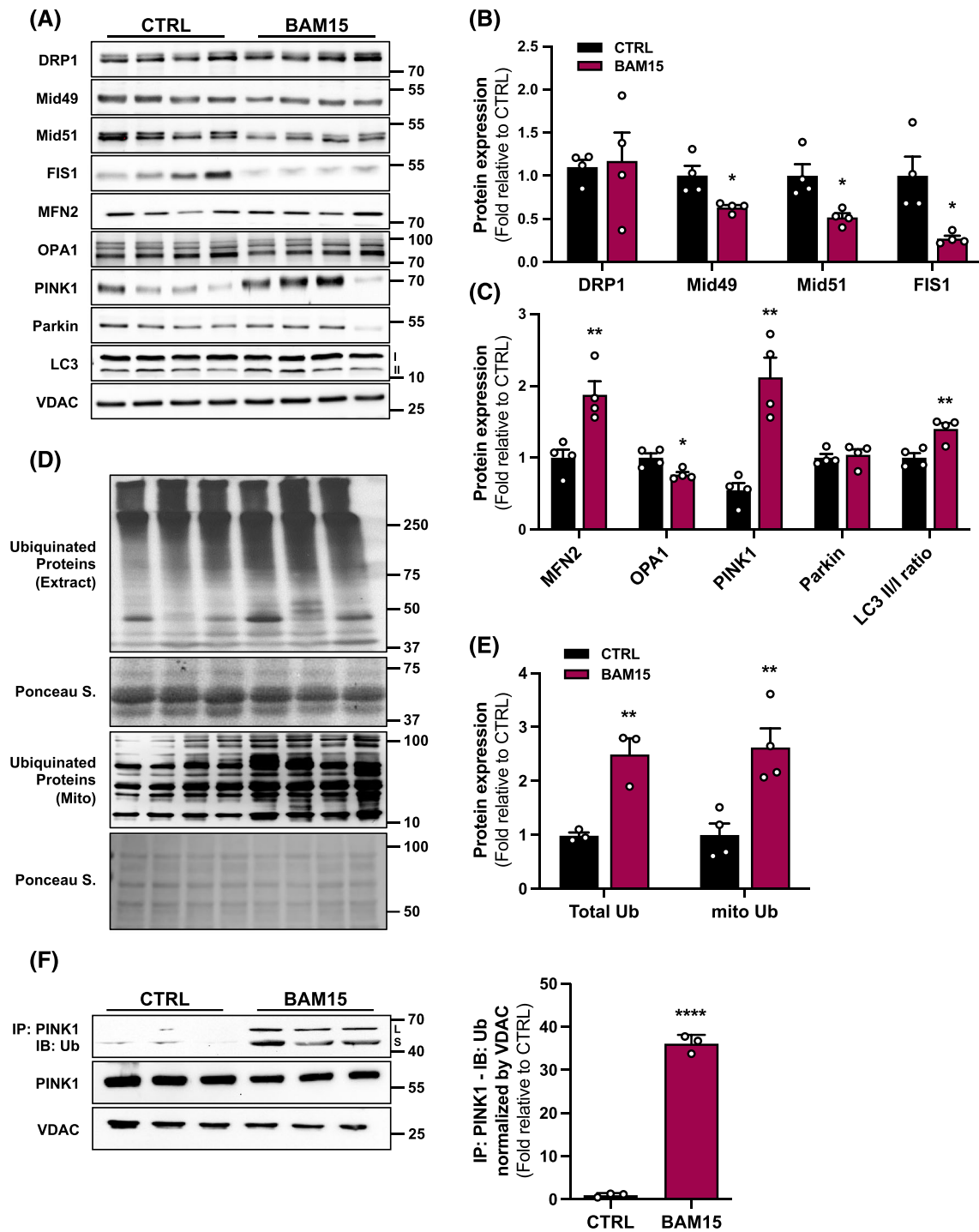


**Figure 5** Mitochondrial uncoupling enhances skeletal muscle mitochondrial function by increasing quality control and network surveillance in aged mice. (A) Representative bands of DRP1, Mid49, Mid51, FIS1, MFN2, OPA1, PINK1, Parkin, LCIII, and VDAC in isolated mitochondria from tissue extracts and (B–C) quantification of protein expression. (D) Representative bands of ubiquitinated proteins in total lysates and mitochondrial fraction and Ponceau S. stain and (E) quantification of protein expression. (F) Protein–protein interaction between PINK1 and ubiquitin (input: PINK1, immunoblot: ubiquitinated proteins) and quantification. Panels (B), (C), (E), and (F) were assessed by unpaired Student’s *t*-test. \**P* < 0.05, \*\**P* < 0.01, and \*\*\*\**P* < 0.0001 indicate statistical significance for between-group comparisons, respectively.

treatment increased the soluble but decreased the insoluble misfolded protein isomer amyloid 11 (A11) oligomer as well as decreased the insoluble/soluble fraction ratio, indicative of a net decrease in ER misfolded proteins (Figure 6C–D). We then examined cytochrome C expression and intracellular localization, which is retained by intact mitochondria and released in response to stress and injury.<sup>23</sup> BAM15 decreased cytochrome C release, evidenced by decreased expression in the cytosol and increased retention by the mitochondria (Figure 6E–F). Moreover, we observed decreased activation of both the initiator Caspase-9 as well as an executioner Caspase-3 following BAM15 compared with CTRL (Figure 6G–H).

Caspase-3 is a protease that interacts with the ubiquitin-proteasome system to stimulate muscle protein degradation by cleaving the actin-myosin complex (called actomyosin) and accelerating protein degradation.<sup>24</sup> To confirm whether the observed reduction in Caspase-3 activation is associated with a decrease in actomyosin degradation, we determined the presence of insoluble and soluble 14-kDa actin fragment in skeletal muscle. BAM15 increased the soluble and decreased the insoluble 14-kDa actin fragment and decreased the insoluble/soluble fraction ratio (Figure 7A–B). Similarly, BAM15 downregulated expression of skeletal muscle atrophy-associated markers, the muscle RING-finger protein-1 (*MuRF1*) and *Atrogin-1* but did not alter expression of myostatin (*MSTN*) compared with CTRL (Figure 7C). Taken together, BAM15 decreases skeletal muscle ER stress response and apoptotic signalling, mediated in part by enhanced cytochrome C retention and ER-protein folding, thus attenuating muscle degradation.

## Discussion

Sarcopenia and obesity have overlapping pathophysiological ramifications that diminish health span.<sup>4,16</sup> Although ageing and obesity are both characterized by impaired skeletal muscle mitochondrial function and chronic inflammation, the molecular mechanisms linking inflammation to mitochondrial impairments remain poorly understood. Here, we provide the first evidence that mitochondrial uncoupling prevents sarcopenic obesity in aged mice mediated via an inflammation-mitochondria-ER axis (Figure 8). Using BAM15, we found that mitochondrial uncoupling: (1) increased muscle mass and function; (2) stimulated mitochondrial IL-6/STAT3 signalling; (3) increased mitochondrial biogenesis, quality control, and OXPHOS activity; and (4) reduced muscle ER stress, apoptotic signalling, and protein degradation.

Energy imbalance is essential to sarcopenic obesity pathogenesis as ageing is associated with a decline in expenditure, whereas environmental obesity is associated with increased intake. Consistent with previous reports in adolescent mice,<sup>10</sup> BAM15-mediated mitochondrial uncoupling was associated

with increased energy expenditure independent of food intake, in effect restoring energy balance. However, unlike adolescent uncoupling models, we observed that both muscle function and physical activity were also improved. Increased oxygen consumption can result from both on-target uncoupling action as well as indirect effects such as altered behaviour and/or improved muscle function.<sup>25</sup> Given the relatively short half-life of BAM15<sup>10</sup> and rapid uptake into metabolically active tissues,<sup>10,11</sup> it is more likely that increased dark phase energy expenditure is explained solely by uncoupling-mediated thermogenesis and that the increase in locomotor function occurred as a secondary effect of decreased body weight and increased muscle mass.

Chronic low-grade inflammation in the context of ageing, coined ‘inflammaging’, accelerates the biological ageing process and is exacerbated by obesity, stimulating overproduction of pro-inflammatory cytokines such as TNF- $\alpha$  or IL-6.<sup>23,26</sup> In previous investigations, we observed that BAM15 decreased systemic markers of inflammation, which was observed in concert with improved liver health and decreased adiposity.<sup>10,11</sup> Chronically elevated IL-6 is associated with muscle wasting, loss of muscle function, and mortality in the elderly.<sup>27</sup> In muscle stem cells, IL-6 is produced by maturing myofibres and is required for hypertrophy.<sup>28</sup> In contrast, IL-6 production in terminally differentiated myofibres stimulates activation of the nuclear transcription factor STAT3 at the canonical Tyr705 site, thus increasing oxidative stress, whereas loss of mitochondrial STAT3 phosphorylation at the alternative Ser727 site increases instability in electron transfer and decreases mitochondrial respiration.<sup>23</sup> Consistently, we observed that BAM15 decreased muscle IL-6 expression and subsequently reduced STAT3 Tyr705 phosphorylation and increased mitochondrial activated STAT3 Ser727. Mitochondrial STAT3 phosphorylation has been previously shown to be important for maintaining redox balance through regulating the opening of the permeability transition pore (MPTP) and STAT3 import.<sup>29,30</sup> Of note, STAT3 may reside in mitochondria-associated ER membranes (MAMs).<sup>31</sup> As such, BAM15 may increase mitochondria-ER contacts and thus enrich STAT3 activity within the MAM, rather than the mitochondria itself. Importantly, we observed increased electron transfer activity and decreased mitochondrial-related apoptosis in concert with increased STAT3 with BAM15, indicative of attenuation of obesity-induced muscle wasting in aged mice.

While the impact of mitochondrial STAT3 signalling on electron transfer and MPTP opening has been investigated in numerous disease models, the influence on components of mitochondrial quality control remains poorly understood.<sup>32</sup> Mitochondria are dynamic organelles, whose morphology and function are regulated through continuous balancing of fission and fusion processes.<sup>33</sup> For example, genetic ablation or overexpression of DRP1, the primary mediator of mitochondrial fission, impairs skeletal muscle integrity, induces muscle wasting, and diminishes metabolic control

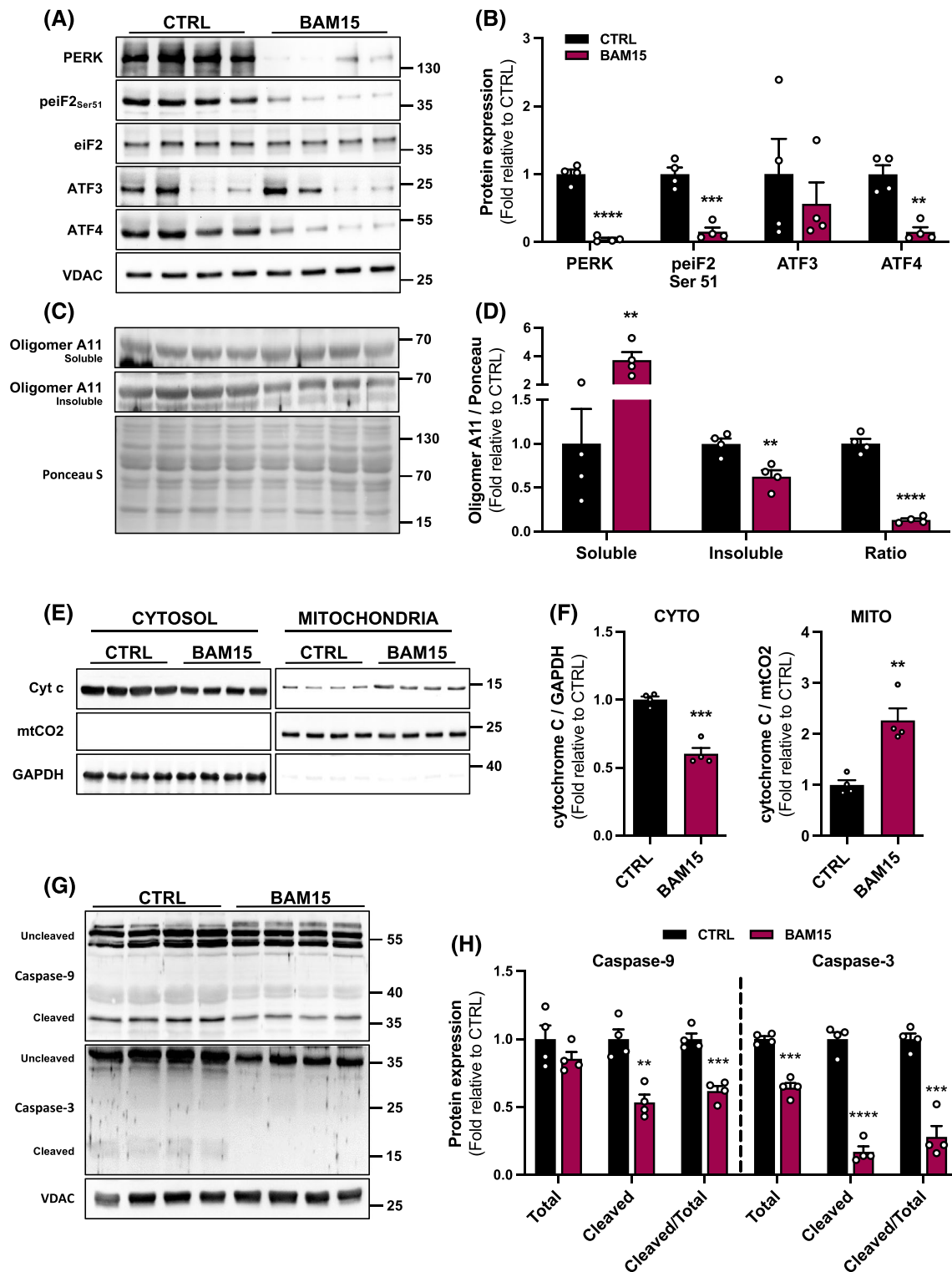


**Figure 6** Mitochondrial uncoupling reduces skeletal muscle endoplasmic reticulum (ER) stress and apoptotic signalling in aged mice. (A) Representative bands of PERK,  $\text{eif2}_{\text{Ser51}}$ , total eIF2, ATF3, ATF4, and VDAC and (B) quantification of protein expression. (C) Representative bands of oligomer A11 expression in the soluble and insoluble fractions and Ponceau S. stain and (D) quantification of protein expression (insoluble/soluble fraction ratio). (E) Representative bands of cytochrome C in the cytosolic and mitochondrial compartments, mtCO2 and GAPDH and (F) quantification of protein expression. (G) Representative bands of uncleaved and cleaved caspase-9, caspase-3, and VDAC and (H) quantification of protein expression. Panels (B), (D), (F), and (H) were assessed by paired Student's *t*-test. \*\* $P < 0.01$ , \*\*\* $P < 0.001$ , and \*\*\*\* $P < 0.0001$  indicate statistical significance for between-group comparisons, respectively.

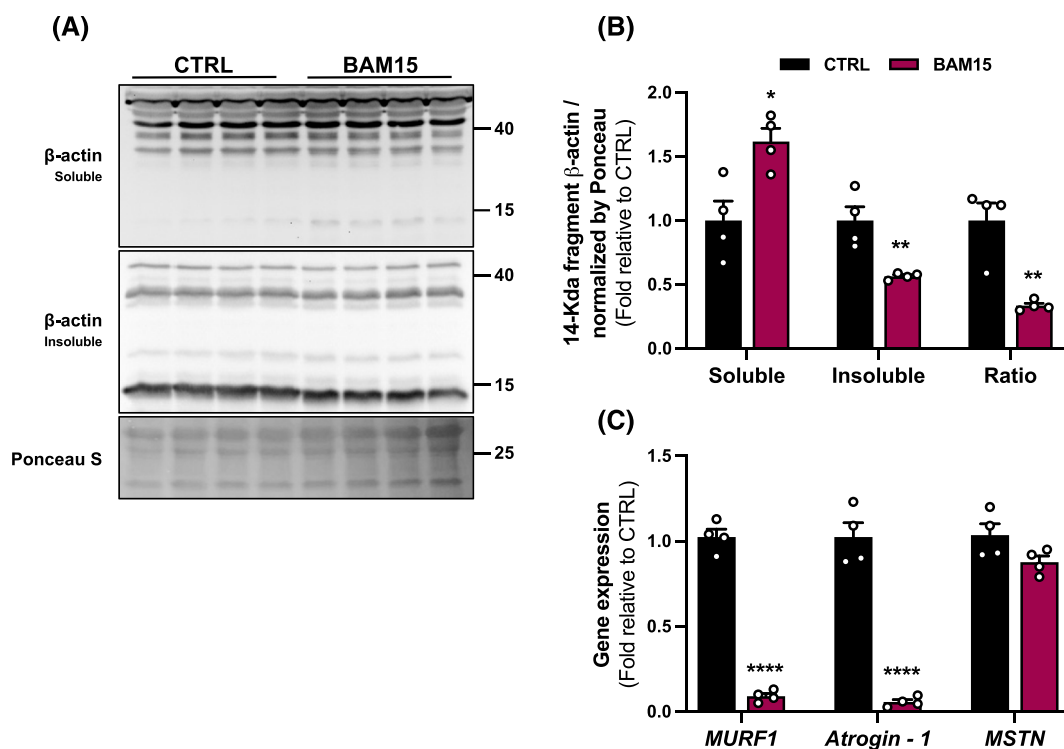


**Figure 7** Mitochondrial uncoupling reduces skeletal muscle protein degradation in aged mice. (A) Representative bands of soluble and insoluble 14-kDa  $\beta$ -actin fragment and Ponceau S. stain in tissue extracts and (B) quantification of protein expression (insoluble/soluble fraction ratio). (C) Gene expression of *MURF1*, *Atrogin-1*, and *myostatin (MSTN)* normalized to  $\beta$ -actin. Panels (B) and (C) were assessed by unpaired Student's *t*-test. \*\* $P < 0.01$ , \*\*\* $P < 0.001$ , and \*\*\*\* $P < 0.0001$  indicate statistical significance for between-group comparisons, respectively.

throughout the lifespan.<sup>34,35</sup> We found that BAM15 reduced mitochondrial fission in aged muscle indirectly by lowering expression of MiD49/51 and FIS1, the proteins responsible for DRP1 binding and docking on the outer mitochondrial membrane.<sup>36</sup> Importantly, restricting receptor/adaptor activity prevents excessive fission and generation of dysfunctional mitochondria while allowing routine fission to occur.<sup>37</sup> BAM15 increased the outer mitochondrial membrane fusion protein, MFN2, but decreased the inner mitochondrial membrane fusion protein, OPA1, indicating that BAM15 did not stimulate mitochondrial fusion activity but likely improved mitochondrial networking contacts.

Parallel to reductions in inflammation and improved mitochondrial networks, BAM15 protected against muscle wasting, mitochondrial content loss, and dysregulated mitophagy. Sarcopenia is consistently observed to produce upregulation of catabolic pathways resulting in increased protein degradation, decreased mitochondrial biogenesis, and impaired autophagy.<sup>4</sup> Specifically, sarcopenic obesity can decrease AMPK activity and its downstream transcription regulator PGC-1 $\alpha$ , both linked with mitochondrial dysfunction in the muscle.<sup>38</sup> We found that BAM15 reduced protein degradation and increased mitochondrial biogenesis through an AMPK-stimulated PGC-1 $\alpha$  axis resulting in downregulation

of the muscle-wasting effects of FoxO3-stimulated transcription of key atrogenes.<sup>39</sup> Additionally, BAM15 increased mitophagy through the AMPK/PINK1/LC3II pathway. Notably, this increase in mitophagy was not mediated through an increase in Parkin, which suggests improved detection of uncoupled, depolarized mitochondria through PINK1 recruitment and accumulation.<sup>40</sup> Parkin may then be selectively recruited from the cytosol to PINK1 flagged-damaged mitochondria and ubiquitinate mitochondrial proteins and recruit autophagosomes.<sup>40</sup> Prototype mitochondrial uncouplers such as FCCP or CCCP rapidly depolarize mitochondrial membrane potential, leading to PINK1 accumulation primarily in the long, uncleaved form (~63 kDa), with only minimal expression of the shortened, processed form (~50 kDa).<sup>40</sup> Conversely, we found that BAM15 increased the expression of the processed, short form of PINK1 in the mitochondria as well as increased ubiquitination suggesting that PINK1 may have been rapidly turned over by proteolysis in the remaining, healthy mitochondria and reintegrated into the network.<sup>41,42</sup>

In addition to reduced protein degradation, BAM15 decreased the presence of misfolded proteins and decreased intrinsic apoptosis. Obesity and ageing induce widespread cellular stress, leading to the accumulation of unfolded or misfolded proteins within the muscle ER lumen, activation

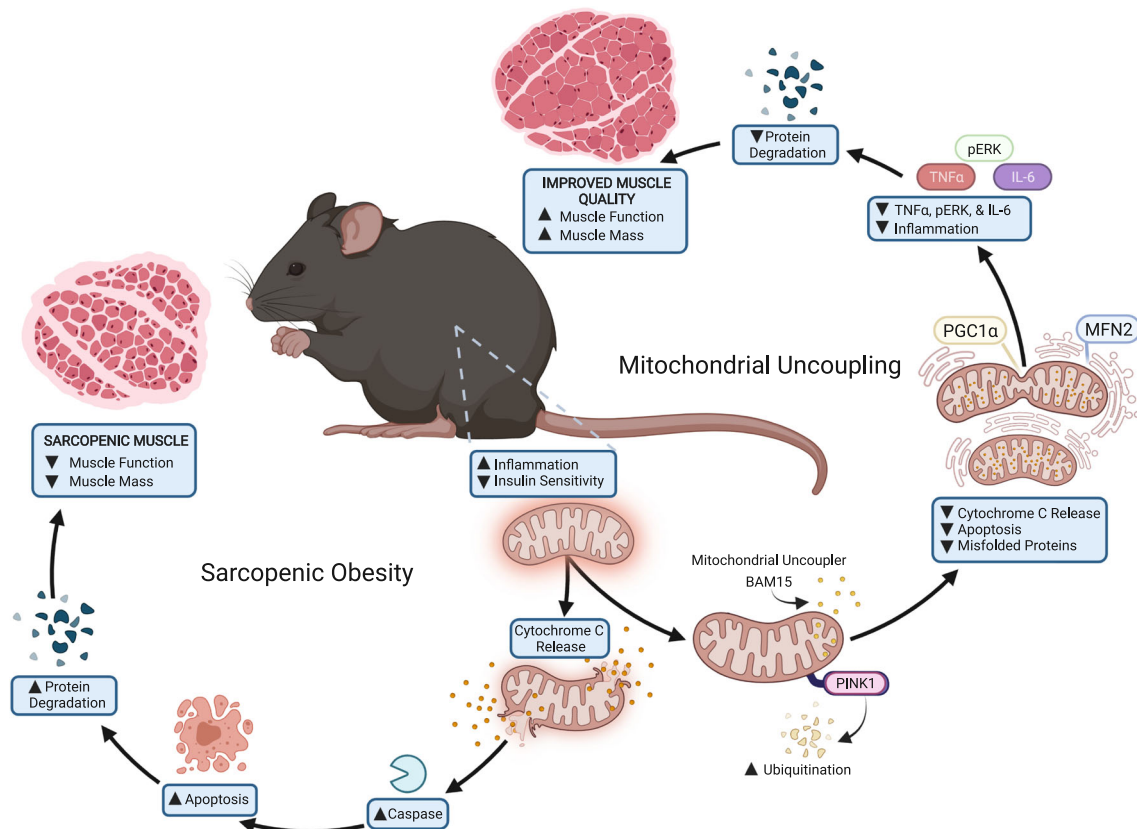


**Figure 8** Working model of mitochondrial uncoupling-mediated attenuation of sarcopenic obesity in aged mice. Ageing in the context of obesity accelerates skeletal muscle mitochondrial damage via chronic inflammation and insulin resistance. The release of cytochrome C from damaged mitochondria triggers activation of caspase-mediated apoptosis, increasing the rate of protein degradation and over time, resulting in diminished muscle mass and function. Mitochondrial uncoupling preserves muscle mass and function by enhancing mitochondrial quality control, biogenesis, and fusion. Improving mitochondrial fitness restricts the release of cytochrome C and activation of intrinsic apoptotic signalling, improving networking with endoplasmic reticulum, and subsequently decreasing muscular inflammation and improving muscle quality.

of apoptosis, and eventual death of the muscle cell.<sup>4,22</sup> Importantly, cell fate is intricately linked to mitochondrial-ER network health and communication through physical contacts, known as the mitochondria-associated membrane (MAM).<sup>21</sup> The outer mitochondrial membrane fusion protein MFN2 is also a master regulator of MAMs serving as a tether of ER-mitochondrial coupling.<sup>21</sup> Previous data suggest that MFN2 expression modulates ER stress and that reduced MFN2 decreases mitochondrial-ER contacts and triggers ER stress.<sup>21</sup> In this view, BAM15 may increase MFN2 expression and enhance the ER-mitochondria contact by improving myocyte adaptation to stress, enhancing the mitochondrial  $\text{Ca}^{2+}$  overload control in the muscle, and ultimately limit or prevent apoptosis. Indeed, BAM15 decreased the mitochondrial cytochrome C release into the cytosol as well as mitochondrial-related apoptotic cascade. Importantly, Caspase-3 is a protease that interacts with the ubiquitin-proteasome system to stimulate muscle protein degradation by cleaving actomyosin, creating a 14-kDa actin proteolytic 'footprint'.<sup>24</sup> Interestingly, muscle

wasting may also be exacerbated by canonical STAT3 phosphorylation at Tyr705, which further stimulates Caspase-3 activation.<sup>24</sup> We observed that the BAM15-induced switch from canonical to noncanonical IL-6/STAT3 signalling is linked with a decrease in cleaved Caspase-3 expression and culminated in a reduction of the muscle-wasting 'footprint'.

In summary, we demonstrate that mitochondrial uncoupling decreases muscle inflammation and enhances mitochondrial-ER network health, which confers protection against sarcopenic obesity in aged mice. Promisingly, BAM15 effectively protected against the loss of muscle mass and function with additional improvements in overall metabolic health. Taken together, prolonged mitochondrial uncoupling induces noncanonical STAT3 signalling, promotes mitochondrial turnover, reduces ER stress, and decreases apoptosis-mediated muscle degradation in skeletal muscle. More broadly, these data highlight that mitochondrial uncouplers may play an important role in improving health span in advanced age.

## Acknowledgements

We thank the CBBC Facility for support with tissue sample processing for histology. We thank the CBC staff for animal care. The authors of this manuscript certify that they comply with the ethical guidelines for authorship and publishing in the *Journal of Cachexia, Sarcopenia and Muscle*.<sup>43</sup>

## Funding

This work used core facilities that are supported in part by COBRE (NIH 5P30GM118430 and 1P20GM135002) and NORC (NIH P30DK072476) Center grants from the National Insti-

tutes of Health. This research was supported in part by the National Institutes of Health [grant U54GM104940 (JPK)].

## Conflict of interest

The authors report no conflicts of interest related to this work.

## Online supplementary material

Additional supporting information may be found online in the Supporting Information section at the end of the article.

## References

- Nations U. *World Population Ageing 2020 Highlights: Living Arrangements of Older Persons*. 2020. <https://www.un.org/development/desa/pd/news/world-population-ageing-2020-highlights>
- Chomentowski P, Dube JJ, Amati F, Stefanovic-Racic M, Zhu S, Toledo FG, et al. Moderate exercise attenuates the loss of skeletal muscle mass that occurs with intentional caloric restriction-induced weight loss in older, overweight to obese adults. *J Gerontol A Biol Sci Med Sci* 2009; **64**:575–580.
- Bachettini NP, Bielemann RM, Barbosa-Silva TG, Menezes AMB, Tomasi E, Gonzalez MC. Sarcopenia as a mortality predictor in community-dwelling older adults: a comparison of the diagnostic criteria of the European Working Group on Sarcopenia in Older People. *Eur J Clin Nutr* 2020; **74**:573–580.
- Batsis JA, Villareal DT. Sarcopenic obesity in older adults: aetiology, epidemiology and treatment strategies. *Nat Rev Endocrinol* 2018; **14**:513–537.
- Porter C, Hurren NM, Cotter MV, Bhattarai N, Reidy PT, Dillon EL, et al. Mitochondrial respiratory capacity and coupling control decline with age in human skeletal muscle. *Am J Physiol Endocrinol Metab* 2015; **309**:E224–E232.
- Sharma A, Smith HJ, Yao P, Mair WB. Causal roles of mitochondrial dynamics in longevity and healthy aging. *EMBO Rep* 2019; **20**:e48395.
- Salvestrini V, Sell C, Lorenzini A. Obesity may accelerate the aging process. *Front Endocrinol* 2019; **10**.
- Klaus S, Ost M. Mitochondrial uncoupling and longevity—a role for mitokines? *Exp Gerontol* 2020; **130**:110796.
- Ulgherait M, Chen A, McAllister SF, Kim HX, Delventhal R, Wayne CR, et al. Circadian regulation of mitochondrial uncoupling and lifespan. *Nat Commun* 2020; **11**:1927.
- Axelrod CL, King WT, Davuluri G, Noland RC, Hall J, Hull M, et al. BAM15-mediated mitochondrial uncoupling protects against obesity and improves glycemic control. *EMBO Mol Med* 2020; **12**:e12088.
- Alexopoulos SJ, Chen SY, Brandon AE, Salamoun JM, Byrne FL, Garcia CJ, et al. Mitochondrial uncoupler BAM15 reverses diet-induced obesity and insulin resistance in mice. *Nat Commun* 2020; **11**:2397.
- Jha P, Wang X, Auwerx J. Analysis of mitochondrial respiratory chain supercomplexes using blue native polyacrylamide gel electrophoresis (BN-PAGE). *Curr Protoc Mouse Biol* 2016; **6**:1–14.
- Dantas WS, Roschel H, Murai IH, Gil S, Davuluri G, Axelrod CL, et al. Exercise-induced increases in insulin sensitivity after bariatric surgery are mediated by muscle extracellular matrix remodeling. *Diabetes* 2020; **69**:1675–1691.
- Hoppel CL, Kerr DS, Dahms B, Roessmann U. Deficiency of the reduced nicotinamide adenine dinucleotide dehydrogenase component of complex I of mitochondrial electron transport. Fatal infantile lactic acidosis and hypermetabolism with skeletal-cardiac myopathy and encephalopathy. *J Clin Invest* 1987; **80**:71–77.
- Mina AI, LeClair RA, LeClair KB, Cohen DE, Lantier L, Banks AS. CalR: a web-based analysis tool for indirect calorimetry experiments. *Cell Metab* 2018; **28**:656, e1–666.
- Kalinkovich A, Livshits G. Sarcopenic obesity or obese sarcopenia: a cross talk between age-associated adipose tissue and skeletal muscle inflammation as a main mechanism of the pathogenesis. *Ageing Res Rev* 2017; **35**:200–221.
- Tan Q, Huang Q, Ma YL, Mao K, Yang G, Luo P, et al. Potential roles of IL-1 subfamily members in glycolysis in disease. *Cytokine Growth Factor Rev* 2018; **44**:18–27.
- Belizário JE, Fontes-Oliveira CC, Borges JP, Kashiabara JA, Vannier E. Skeletal muscle wasting and renewal: a pivotal role of myokine IL-6. *Springerplus* 2016; **5**:619.
- Wegrzyn J, Potla R, Chwae YJ, Sepuri NB, Zhang Q, Koeck T, et al. Function of mitochondrial Stat3 in cellular respiration. *Science* 2009; **323**:793–797.
- Lopez-Otin C, Blasco MA, Partridge L, Serrano M, Kroemer G. The hallmarks of aging. *Cell* 2013; **153**:1194–1217.
- Rowland AA, Voeltz GK. Endoplasmic reticulum–mitochondria contacts: function of the junction. *Nat Rev Mol Cell Biol* 2012; **13**:607–615.
- Deldicque J, Cani PD, Philp A, Raymackers LM, Meakin PJ, Ashford ML, et al. The unfolded protein response is activated in skeletal muscle by high-fat feeding: potential role in the downregulation of protein synthesis. *Am J Physiol Endocrinol Metab* 2010; **299**:E695–E705.
- Abid H, Ryan ZC, Delmotte P, Sieck GC, Lanza IR. Extramyocellular interleukin-6 influences skeletal muscle mitochondrial physiology through canonical JAK/STAT signaling pathways. *FASEB J* 2020; **34**:14458–14472.
- Silva KA, Dong J, Dong Y, Schor N, Tweardy DJ, et al. Inhibition of Stat3 activation suppresses caspase-3 and the ubiquitin-proteasome system, leading to preservation of muscle mass in cancer cachexia. *J Biol Chem* 2015; **290**:11177–11187.
- Demine S, Renard P, Arnould T. Mitochondrial uncoupling: a key controller of biological processes in physiology and diseases. *Cell* 2019; **8**:795.
- Salminen A, Kaarniranta K, Kauppinen A. Inflammaging: disturbed interplay between autophagy and inflammasomes. *Ageing (Albany NY)* 2012; **4**:166–175.
- Puzianowska-Kuznicka M, Owczarzewicz M, Wieczorowska-Tobis K, Nadrowski P, Chudek J, Slusarczyk P, et al. Interleukin-6 and C-reactive protein, successful aging, and mortality: the PolSenior study. *Immun Ageing* 2016; **13**:21.

28. Serrano AL, Baeza-Raja B, Perdiguero E, Jardi M, Munoz-Canoves P. Interleukin-6 is an essential regulator of satellite cell-mediated skeletal muscle hypertrophy. *Cell Metab* 2008;**7**:33–44.
29. Baines CP, Kaiser RA, Purcell NH, Blair NS, Osinska H, Hambleton MA, et al. Loss of cyclophilin D reveals a critical role for mitochondrial permeability transition in cell death. *Nature* 2005;**434**:658–662.
30. Tamminen P, Anugula C, Mohammed F, Anjaneyulu M, Larner AC, Sepuri NB. The import of the transcription factor STAT3 into mitochondria depends on GRIM-19, a component of the electron transport chain. *J Biol Chem* 2013;**288**:4723–4732.
31. Su Y, Huang X, Huang Z, Huang T, Xu Y, Yi C. STAT3 localizes in mitochondria-associated ER membranes instead of in mitochondria. *Front Cell Dev Biol* 2020;**8**.
32. Meier JA, Larner AC. Toward a new STATE: the role of STATs in mitochondrial function. *Semin Immunol* 2014;**26**:20–28.
33. Chan DC. Fusion and fission: interlinked processes critical for mitochondrial health. *Annu Rev Genet* 2012;**46**:265–287.
34. Dulac M, Leduc-Gaudet JP, Cefis M, Ayoub MB, Reynaud O, Shams A, et al. Regulation of muscle and mitochondrial health by the mitochondrial fission protein Drp1 in aged mice. *J Physiol* 2021;**599**:4045–4063.
35. Axelrod CL, Fealy CE, Erickson ML, Davuluri G, Fujioka H, Dantas WS, et al. Lipids activate skeletal muscle mitochondrial fission and quality control networks to induce insulin resistance in humans. *Metabolism* 2021;**121**:154803.
36. Fealy CE, Grevendonk L, Hoeks J, Hesselink MKC. Skeletal muscle mitochondrial network dynamics in metabolic disorders and aging. *Trends Mol Med* 2021. <https://doi.org/10.1016/j.molmed.2021.07.013>
37. Benard G, Bellance N, James D, Parrone P, Fernandez H, Letellier T, et al. Mitochondrial bioenergetics and structural network organization. *J Cell Sci* 2007;**120**:838–848.
38. Huang Y, Zhu X, Chen K, Lang H, Zhang Y, Hou P, et al. Resveratrol prevents sarcopenic obesity by reversing mitochondrial dysfunction and oxidative stress via the PKA/LKB1/AMPK pathway. *Aging (Albany NY)* 2019;**11**:2217–2240.
39. Sandri M, Lin J, Handschin C, Yang W, Arany ZP, Lecker SH, et al. PGC-1alpha protects skeletal muscle from atrophy by suppressing FoxO3 action and atrophy-specific gene transcription. *Proc Natl Acad Sci U S A* 2006;**103**:16260–16265.
40. Matsuda N, Sato S, Shiba K, Okatsu K, Saisho K, Gautier CA, et al. PINK1 stabilized by mitochondrial depolarization recruits Parkin to damaged mitochondria and activates latent Parkin for mitophagy. *J Cell Biol* 2010;**189**:211–221.
41. Kawajiri S, Saiki S, Sato S, Sato F, Hatano T, Eguchi H, et al. PINK1 is recruited to mitochondria with Parkin and associates with LC3 in mitophagy. *FEBS Lett* 2010;**584**:1073–1079.
42. Kim Y, Park J, Kim S, Song S, Kwon SK, Lee SH, et al. PINK1 controls mitochondrial localization of Parkin through direct phosphorylation. *Biochem Biophys Res Commun* 2008;**377**:975–980.
43. von Haehling S, Morley JE, Coats AJS, Anker SD. Ethical guidelines for publishing in the Journal of Cachexia, Sarcopenia and Muscle: update 2021. *J Cachexia Sarcopenia Muscle* 2021;**12**:2259–2261.